# THE ESTABLISHMENT OF TYPICAL DOSE AND ASSESSMENT OF SCANNING PARAMETERS INFLUENCING RADIATION DOSE IN CARDIAC COMPUTED TOMOGRAPHY (CT) IMAGING

# NUR SYAHIRA BINTI SOLEHUDDIN

# SCHOOL OF HEALTH SCIENCES UNIVERSITI SAINS MALAYSIA

# THE ESTABLISHMENT OF TYPICAL DOSE AND ASSESSMENT OF SCANNING PARAMETERS INFLUENCING RADIATION DOSE IN CARDIAC COMPUTED TOMOGRAPHY (CT) IMAGING

by

# NUR SYAHIRA BINTI SOLEHUDDIN

Dissertation submitted in partial fulfilment of the requirements for the degree of Bachelor of Medical Radiation (Honours)

#### **CERTIFICATE**

This is to certify that the dissertation entitled "THE ESTABLISHMENT OF TYPICAL DOSE AND ASSESSMENT OF SCANNING PARAMETERS INFLUENCING RADIATION DOSE IN CARDIAC COMPUTED TOMOGRAPHY (CT) IMAGING" is a bona fide record of research work conducted by Ms. Nur Syahira binti Solehuddin (159170) during the period from October 2024 to July 2025 under our supervision. We have read this dissertation and, in our opinion, it meets the acceptable standards of scholarly presentation and is adequate in both scope and quality. This dissertation is submitted in partial fulfilment of the requirements for the degree of Bachelor of Medical Radiation (Honours).

	$\sim$	•
Maın	Sup	ervisor,

Co-Supervisor,

Field Supervisor,

Assoc. Prof. Dr. Diyana

binti Osman,

Department of

Biomedical Imaging,

Advanced Medical and

Dental Institute (IPPT),

Universiti Sains Malaysia

13200 Kepala Batas,

Pulau Pinang, Malaysia

Assoc. Prof. Dr. Khairil Amir

Bin Sayuti,

Head, Department of

Radiology,

School of Medical Sciences,

Universiti Sains Malaysia

Jalan Raja Perempuan Zainab

II, 16150 Kubang Kerian,

Kelantan, Malaysia

Pn. Norfataha Binti

Mohd Daud

Radiographer U42

Department of Radiology

Hospital Universiti Sains

Malaysia,

16150 Kubang Kerian,

Kelantan, Malaysia

Date: 30/06/2025

**DECLARATION** 

I hereby declare that this dissertation is the result of my own investigations, except where

otherwise stated and duly acknowledged. I also declare that it has not been previously or

concurrently submitted as a whole for any other degrees at Universiti Sains Malaysia or

other institutions. I grant Universiti Sains Malaysia the right to use the dissertation for

teaching, research and promotional purposes.

Syahira Solehudddin

Nur Syahira binti Solehuddin,

Date: 23/06/2025

2

#### **ACKNOWLEDGEMENT**

Alhamdulillah, all praise be to Allah SWT for granting the strength, patience, and guidance in completing this final year project.

The deepest appreciation is extended to the main supervisor, Assoc. Prof. Dr. Diyana binti Osman, for the invaluable guidance, encouragement, and continuous support throughout the research period. Sincere thanks are also conveyed to the co-supervisor, Assoc. Prof. Dr. Khairil Amir Bin Sayuti, for the constructive input and expert advice given throughout the study.

Gratitude is also due to the field supervisor, Puan Norfataha binti Mohd Daud, for the support and assistance during the data collection process at the Department of Radiology, Hospital Pakar Universiti Sains Malaysia (HPUSM). Appreciation is extended to the radiology staff and PACS team at HPUSM for the cooperation and facilitation provided during this research, whose work allowed this study to be carried out effectively.

The highest gratitude is also dedicated to the beloved parents and family for the endless prayers, love, and moral support given throughout this academic journey. Appreciation is also extended to the friends and coursemates for the support, motivation, and encouragement from beginning to end.

Finally, special thanks to Universiti Sains Malaysia (USM) and USM Human Ethical Committee (JEPeM) for the facilities, resources, and approval that made this research possible.

# TABLE OF CONTENTS

CERTIF	ICATE1
DECLA	RATION2
ACKNO	WLEDGEMENT3
TABLE	OF CONTENTS4
ABSTR	AK14
ABSTR	ACT
CHAPT	ER 1
1.1	Background of the Study
1.2	Problem Statement 3
1.3	Objective of Study4
1.3.1	General objective
1.3.2	Specific objectives
1.4	Hypothesis4
1.4.1	Null Hypothesis4
1.4.2	Alternative Hypothesis
1.5	Significance of Study5
1.6	Scope and Limitations6
1.7	Thesis Organisation
CHAPT	ER 28
2.1	Basic Principles of Computed Tomography (CT)
2.1.1	X-ray Attenuation Through an Object
2.1.2	Image Data Acquisition
2.1.3	CT Image Reconstruction
2.1.4	CT Numbers/Hounsfield Units
2.1.5	Components of CT Scanner
2.1.6	Scanning Mode in Cardiac CT
2.2	CT Dosimetry
2.2.1	Computed Tomography Dose Index (CTDI)15
2.2.1	Dose-Length Product (DLP)
2.3	Coronary Computed Tomography Angiography (CCTA)
2.4	Radiation Dose Distribution in Patient Demographic (Age and Gender) 18
2.5	Scanning Parameters Influencing Radiation Dose in CT Imaging

	2.5.1	Exposure Time and Scan Length	. 19
	2.5.2	Tube Current (mA) and Exposure Time (s)	. 20
	2.6	Radiation Dose Management in Cardiac CT	. 21
	2.7	Typical Dose (50th Percentile)	. 22
	2.8	Establishing Local Diagnostic Reference Levels (LDRLs)	. 23
C	CHAPTE	CR 3	. 25
	3.1	Research Tools	. 25
	3.1.1	CT Scanners	. 25
	3.1.2	Radiology Information System (VIARAD5)	. 30
	3.1.3	Pictures Archiving and Communication System	. 31
	3.1.4	Microsoft Excel 2021	. 32
	3.2	Research Methodology	. 33
	3.2.1	Research Design	. 33
	3.2.2	Study Flowchart	. 34
	3.2.3	Study Location and Duration	. 34
	3.2.4	Study Population and Sample	. 35
	3.2.5	Sampling Method	. 35
	3.2.6	Selection Criteria	. 36
	3.2.6.1	Inclusion Criteria	. 36
	3.2.6.2	Exclusion Criteria	. 36
	3.2.7	Sample Size Calculation	. 37
	3.2.8	Data Collection	. 38
	3.2.9	Data Analysis	. 39
C	CHAPTE	CR 4	. 42
	4.1	Patient Demographic	. 43
	4.2	Radiation Dose Distribution in Cardiac CT Imaging	. 44
	4.2.1	Based on CT Protocol	. 44
	4.2.2	Based on Age Groups	. 51
	4.2.3	Based on Gender	. 57
	4.3 Imagin	Influence of Scanning Parameters on Radiation Dose in Tomography (C	
	4.3.1	Tube current–time product (mAs)	
	4.3.2	Exposure Time	
	4.3.3	Scan Length	
	4.4	Establishment of Typical Dose for Local Diagnostic Reference Level (LDF	
	in Card	liac CT Imaging in Hospital Pakar Universiti Sains Malaysia	
		5	

CHAPTER 5		80
5.1	Conclusion	80
5.2	Limitation of Study	82
5.3	Recommendation for Future Research	82
REFERE	ENCE	84
APPENI	DICES	87
Appen	ndices A: JEPeM Ethical Approval Letter	87
Appen	ndices B: Data Collection	89

# LIST OF TABLES

Table 3.1: The Technical details of the CT scanner used in this research
Table 4.1: Patient demographic used for this research
Table 4.2: Summary of radiation dose distribution across different cardiac CT protocols.
47
Table 4.3: Radiation dose distribution within the age groups in cardiac CT imaging 54
Table 4.4: The average radiation dose for both genders
Table 4.5: Correlation coefficient, r and coefficient of determination, R2 for tube current-
time product (mAs) factor
Table 4.6 : Correlation coefficient, r and coefficient of determination, R <sup>2</sup> for exposure
time (seconds) factor
Table 4.7: Correlation coefficient, r and coefficient of determination, R2 for scan length
(cm) factor
Table 4.8: Summary of scan length across different cardiac CT protocols
Table 4.9: Typical dose for Local Diagnostic Reference Level (LDRL) in cardiac CT
imaging in HPUSM
Table 4.10: Comparison of typical dose and Local Diagnostic Reference Level (LDRL)
values for CTDIvol and DLP across cardiac CT studies

# LIST OF FIGURES

Figure 2.1: X-ray beam attenuations passing through of an object (left) and intensity of
an X-ray beam passing through an object with multiple different linear attenuation
coefficients (μ1, μ2, μ3, μ4) (right) (Jung, 2021)9
Figure 2.2: Range of Hounsfield Unit (HU) scale of computed tomography (CT) numbers
for various tissues (Jung, 2021).
Figure 3.1: Siemens SOMATOM Definition AS+ CT
Figure 3.2: Philips Incisive CT scanner at the Department of Radiology
Figure 3.3: The study flowchart for this research
Figure 4.1: Box-and-whisker plot showing the distribution of CTDIvol (mGy) across
different cardiac CT protocols
Figure 4.2: Box-and-whisker plot showing the distribution of DLP (mGy.cm) across
different cardiac CT protocols
Figure 4.3: Box-and-whisker plot showing the distribution of total DLP per examination
(mGy·cm) across different cardiac CT protocols
Figure 4.4: Box-whisker-plot of CTDI <sub>vol</sub> (mGy) vs Age Group
Figure 4.5: Box-whisker-plot of DLP (mGy.cm) vs Age Group
Figure 4.6: Box-whisker-plot of Total DLP per examination (mGy.cm) vs Age Group. 53
Figure 4.7: Bar chart showing the average CTDI <sub>vol</sub> (mGy) for male and female patients
across two CT scanner types (Siemens and Philips)
Figure 4.8: Bar chart showing the average DLP in mGy·cm for male and female patients
across two CT scanner types (Siemens and Philips)

Figure 4.9: Bar chart showing the average total DLP per examination in mGy·cm for male
and female patients across two CT scanner types (Siemens and Philips)
Figure 4.10: Scatter plots of CTDI <sub>vol</sub> (mGy) vs tube-current time product (mAs) 62
Figure 4.11: Scatter plots of DLP (mGy.cm) vs tube-current time product (mAs) 62
Figure 4.12: Scatter plots of CTDI <sub>vol</sub> (mGy) vs exposure time (seconds)
Figure 4.13: Scatter plots of DLP (mGy.cm) vs exposure time (seconds)
Figure 4.14: Scatter plots of DLP (mGy.cm) vs scan length (cm)70
Figure 4.15: Box-and-whisker plot showing the distribution of scan length (cm) among
different cardiac CT protocols
Figure 6.1: The approval letter received from JEPeM USM for this research
Figure 6.2: A screenshot of Microsoft Excel 2021 containing data extracted from the
VIARAD5 system
Figure 6.3: A screenshot of the PACS interface used for retrieving patient imaging data.
Figure 6.4: A screenshot of patient protocol details for the Siemens SOMATOM
Definition AS+ retrieved from the PACS system. 90
Figure 6.5: A screenshot of patient protocol details for the Philips Incisive CT retrieved
from the PACS system
Figure 6.6: A screenshot of a DICOM image displayed within the PACS interface 91
Figure 6.7: A screenshot of Microsoft Excel 2021 showing the dataset after sorting and
organizing for analysis91

#### LIST OF SYMBOLS

bpm Beats per minute

CTDI<sub>vol</sub> Volume Computed Tomography Dose Index

CTDI<sub>w</sub> Weighted Computed Tomography Dose Index

CTDI<sub>100</sub> Computed Tomography Dose Index over 100 mm

DLP Dose-Length Product

HU Hounsfield Unit

mAs Milliampere-seconds (tube current-time product)

mGy Milligray

s Seconds

cm Centimetres

R<sup>2</sup> Coefficient of Determination

r Pearson Correlation Coefficient

μ Linear Attenuation Coefficient

 $P(r,\theta)$  Projection function (position and angle)

f(x,y) Attenuation function (image reconstruction)

I Intensity of the X-ray beam

#### LIST OF ABBREVIATIONS

AEC Automatic Exposure Control

AIDR3D Adaptive Iterative Dose Reduction 3D (Canon)

ALARA As Low as Reasonably Achievable

AMDI Advanced Medical and Dental Institute

ASIR Adaptive Statistical Iterative Reconstruction

CACS Coronary Artery Calcium Scoring

CARE Dose 4D Combined Applications to Reduce Exposure – Dose Modulation

in 4 Dimensions

CBCT Cone Beam Computed Tomography

CTA Coronary Computed Tomography Angiography

CST Computed Scan Time

CT Computed Tomography

CTDI Computed Tomography Dose Index

CVD Cardiovascular Disease

CorCTA Coronary CT Angiography (Helical, Siemens)

CorCTAAdapt Coronary CT Angiography with Adaptive Sequence (Step-and-

Shoot, Siemens)

DICOM Digital Imaging and Communications in Medicine

DLP Dose Length Product

DLR Deep Learning Reconstruction

DRL Diagnostic Reference Level

ECG Electrocardiogram

FBP Filtered Back Projection

FOV Field of View

F Female

HPUSM Hospital Pakar Universiti Sains Malaysia

HU Hounsfield Unit

ICRP International Commission on Radiological Protection

IDose<sup>4</sup> Iterative Dose Optimisation Software – Fourth Generation

IR Iterative Reconstruction

IRIS Iterative Reconstruction in Image Space (Siemens)

IQR Interquartile Range

JEPeM Jawatankuasa Etika Penyelidikan Manusia (USM Human Ethical

Committee)

KFCH King Fahad Central Hospital

LDRL Local Diagnostic Reference Level

M Male

MDCT Multi-Detector Computed Tomography

MSCT Multi-Slice Computed Tomography

NaI Sodium Iodide (Scintillation Detector)

NDRL National Diagnostic Reference Level

PACS Picture Archiving and Communication System

PMMA Polymethyl Methacrylate (Phantom Material)

RIS Radiology Information System

ROSe Reconstruction on the Scanner Engine (Philips)

SD Standard Deviation

TAP Thorax Abdomen Pelvis

TAVI Transcatheter Aortic Valve Implantation

UFC Ultrafast Ceramic

vMRC

Voltage-Controlled Medical Rotating Cathode (Performance X-ray Tube, Siemens)

#### LIST OF APPENDICES

Appendices A – JEPeM Ethical Approval

Appendices B – Data Collection

#### LIST OF EQUATIONS

Equation 1: Beer–Lambert Law describing how X-ray intensity is attenuated as it passes through a material (Jung, 2021).

Equation 2: Beer–Lambert Law used in CT imaging to represent X-ray attenuation through multiple tissues or materials, each with a different linear attenuation coefficient (Jung, 2021).

Equation 3: CT Number (HU) (Jung, 2021).

Equation 4: Dose-Length Product (Zhao et al., 2022).

Equation 5: The formula used to obtain sample size value (Asenahabi and Ikoha, 2023).

#### PENETAPAN DOS TIPIKAL DAN PENILAIAN PARAMETER PENGIMBASAN

#### YANG MEMPENGARUHI DOS SINARAN DALAM PENGIMEJAN

#### TOMOGRAFI BERKOMPUTER (CT) JANTUNG

#### **ABSTRAK**

Tomografi berkomputer (CT) jantung digunakan secara meluas untuk mengesan penyakit arteri koronari, namun melibatkan pendedahan radiasi yang tinggi dan memerlukan pengoptimuman. Kajian ini bertujuan menentukan aras dos tipikal dan menilai parameter imbasan yang mempengaruhi variasi dos dalam CT jantung di HPUSM. Sebanyak 200 kes dianalisis secara retrospektif daripada pengimbas CT Siemens dan Philips. Data demografi dan teknikal seperti mAs, masa dedahan, panjang imbasan, CTDI vol, dan DLP diperoleh daripada sistem PACS dan VIARAD5, dan dianalisis menggunakan Microsoft Excel 2021. CorCTAAdapt mencatatkan dos terendah, manakala CTA Koronari menunjukkan nilai tertinggi. Terdapat korelasi positif antara mAs, masa dedahan dan panjang imbasan dengan CTDIvol dan DLP. Dos tipikal ditentukan melalui peratusan ke-50, manakala peratusan ke-75 digunakan untuk menetapkan LDRL. Dos tipikal masingmasing ialah 17.39 mGy/233.00 mGy·cm (CorCTA), 16.87 mGy/168.50 mGy·cm (CorCTAAdapt), dan 48.97 mGy/861.90 mGy·cm (CTA Coronary). Kajian ini berjaya menetapkan nilai dos tipikal serta mengenal pasti parameter imbasan yang mempengaruhi variasi dos dalam imbasan CT jantung. Dapatan ini menyediakan data rujukan tempatan penting untuk pengoptimuman dos dan menyokong pembangunan protokol pengimejan yang lebih selamat dan seragam di HPUSM.

Kata kunci: CT jantung, Dos tipikal, Paras Rujukan Diagnostik, Pengoptimuman dos, Parameter teknikal.

THE ESTABLISHMENT OF TYPICAL DOSE AND ASSESSMENT OF

SCANNING PARAMETERS INFLUENCING RADIATION DOSE IN CARDIAC

COMPUTED TOMOGRAPHY (CT) IMAGING

**ABSTRACT** 

Cardiac computed tomography (CT) is widely used for detecting coronary artery disease

but involves relatively high radiation doses, necessitating optimisation. This study aimed

to determine typical dose levels and assess scanning parameter influencing dose variation

in cardiac CT at HPUSM. A total of 200 cases were retrospectively reviewed from

Siemens SOMATOM Definition AS+ and Philips Incisive CT scanners. Demographic and

technical data, including mAs, exposure time, scan length, CTDI vol, and DLP, were

extracted from PACS and VIARAD5. Microsoft Excel 2021 was used to analyse the

relationship between scan parameters and dose. CorCTAAdapt (Siemens) showed the

lowest dose, while CTA Coronary (Philips) had the highest. Positive correlations were

found between mAs, exposure time, and scan length with CTDIvol and DLP. The 50th

percentile defined the typical dose; the 75th established local diagnostic reference levels

(LDRLs). Typical doses were 17.39 mGy/233.00 mGy·cm (CorCTA), 16.87 mGy/168.50

mGy·cm (CorCTAAdapt), and 48.97 mGy/861.90 mGy·cm (CTA Coronary). This study

established typical dose values and identified key scanning parameters that influence dose

in cardiac CT imaging. The findings offer important local reference data for dose

optimisation and support the development of safer, standardised imaging protocols at

HPUSM.

Keywords: Cardiac CT, Typical Dose, Diagnostic Reference Level, Dose Optimisation,

Technical Parameters

15

#### **CHAPTER 1**

#### INTRODUCTION

#### 1.1 Background of the Study

In Malaysia, CVD is a serious public health concern, ischaemic heart disease is acknowledged as the main cause of death in recent years. Rising frequency of coronary artery disease and acute coronary syndrome has increased demand for non-invasive imaging modalities including heart Computed Tomography (CT), a necessary diagnostic tool for evaluating heart anatomy and spotting vascular abnormalities. High-resolution, three-dimensional imaging of the coronary arteries made possible by cardiac CT—including Coronary CT Angiography (CCTA) and Coronary Artery Calcium Scoring (CACS)—allows early detection and treatment.

Cardiac CT is widely applied in clinical practice for various diagnostic purposes, including evaluating coronary artery stenosis, quantifying total calcium score, and monitoring post-treatment outcomes such as coronary artery bypass grafting and angioplasty. Multi-slice computed tomography (MSCT) also supports structural assessments of heart valves, characterisation of atherosclerotic plaques, and examination of pulmonary vein openings in patients undergoing ablation therapy for atrial fibrillation. Moreover, it facilitates the measurement of key hemodynamic parameters such as end-systolic and end-diastolic volumes, stroke volume, and ejection fraction for both ventricles, along with myocardial mass estimation. CT imaging is additionally critical for procedural planning, including stent graft implantation and transcatheter aortic valve implantation (TAVI), as well as in the evaluation of congenital heart anomalies in both paediatric and adult patients (Piłat et al., 2024).

Moreover, even if cardiac CT is crucial for clinical usage, the excessive and unnecessary radiation exposure remains a cause of worry. Reducing unnecessary exposure and maintaining diagnosis image quality depend on optimising the radiation dosage. In response to increasing global medical radiation exposure, the International Commission on Radiological Protection (ICRP) first introduced the concept of Diagnostic Reference Levels (DRLs) in 1996. This was later reinforced in ICRP Publication 103, which advocated for the establishment of DRLs as a practical tool for dose optimization. Further guidance was provided in ICRP Publication 135, which clarified the definition and methodology for setting DRLs across various imaging modalities (Kahraman et al., 2024). In medical imaging, radiation dosages are measured against Diagnostic Reference Levels (DRLs). DRLs are often established based on the 75th percentile of dose distributions recorded in clinical practice.

The typical dose signifies the most common radiation dose administered during an imaging process, frequently indicated by the median value (50th percentile) of the dose distribution. In contrast to the 75th percentile used for DRLs, a typical dose establishes a benchmark for comprehending standard and common practice and patient exposure under normal conditions. Determining the standard dosage facilitates understanding of dose changes as well as helps in optimising radiation exposure.

The present study aims to establish the typical radiation dose for cardiac CT imaging and assess the scanning parameters influencing dose variations. Scanning parameters such as mAs, exposure time and scan length are evaluated to understand their impact on radiation dose. By analysing patient exposure data, this research will support the optimisation of dose management, promote safer imaging practices, and contribute to the establishment of local DRLs for cardiac CT in HPUSM.

#### 1.2 Problem Statement

Cardiovascular disease (CVD) has been identified as the main cause of death globally, accounting for 17.3% of all fatalities worldwide, with 17.6 million deaths reported in 2016 alone. Early CVD diagnosis and detection are very vital for bettering patient outcomes, easing the pressure on healthcare systems, and lowering of financial burden (Alhailiy, Ekpo et al., 2018). Moreover, because of its precision in offering thorough view of coronary arteries and heart tissues, cardiac CT scan is among the highest dosage tests. Patients having coronary CT angiography (CCTA), for example, usually get radiation doses ranging from 5 to 32 mSv; whereas, doses for a 64-slice coronary CT angiography (CTA) with tube current modulation might range between 12 to 18 mSv. These levels are far higher than those used in conventional chest CT scans, which run between 4 and 18 mSv.

Despite the relevance of cardiac CT in the diagnosis and management of CVD, there remain major challenges in optimizing radiation dose while maintaining diagnostic quality. The absence of established imaging techniques and Diagnostic Reference Levels (DRLs) has led to inconsistencies in the management of radiation doses, specifically in HPUSM. DRLs serve as key benchmarks for comparing radiation doses across different centres and have been demonstrated to minimise radiation exposure by up to 50% when correctly used. However, at HPUSM, the lack of established local DRLs for cardiac CT imaging remains a difficulty in maintaining safe and effective imaging techniques. This inconsistency not only increases the risk of unnecessary radiation exposure to patients but also underscores the necessity for a comprehensive examination of radiation doses and the scanning parameters determining these doses.

Given these challenges, it is important to establish typical dose levels for cardiac CT imaging and assess the scanning parameters that contribute to variations in radiation dose distribution, such as mAs, exposure time and scan length. By addressing these issues, this study aims to optimize radiation dose management, improve patient safety, and promote the implementation of standardized protocols for cardiac CT imaging at HPUSM.

#### 1.3 Objective of Study

#### 1.3.1 General objective

This study aims to establish the typical dose and assess the scanning parameters that influence radiation dose in cardiac CT imaging

#### 1.3.2 Specific objectives

- 1. To determine the radiation dose distribution (clinical protocols, age group and gender) in patients undergoing cardiac CT imaging.
- 2. To study the correlation between scanning parameters (mAs, exposure time and scan length) with radiation dose in cardiac CT imaging.
- To determine the typical dose for local diagnostic reference level (LDRL) in cardiac CT imaging in HPUSM.

#### 1.4 Hypothesis

#### 1.4.1 Null Hypothesis

There is no correlation between scanning parameters (mAs, exposure time and scan length) with radiation dose in cardiac CT imaging.

#### 1.4.2 Alternative Hypothesis

There is correlation between scanning parameters (mAs, exposure time and scan length) with radiation dose in cardiac CT imaging.

#### 1.5 Significance of Study

This study is important in advancing safer and more effective practices in cardiac CT imaging. With cardiovascular disease (CVD) continuing to be the leading cause of death in Malaysia and around the world, the use of cardiac CT—particularly Coronary CT Angiography (CCTA) and Coronary Artery Calcium Scoring (CACS)—has become increasingly common due to its accuracy and non-invasive nature. However, these benefits come with the drawback of relatively high radiation doses, which can pose risks to patient safety, especially with repeated exposure.

The significance of this study lies in its effort to establish typical radiation dose values and identify the scanning parameters that influence dose levels in cardiac CT. This is particularly relevant for HPUSM, where local Diagnostic Reference Levels (DRLs) for cardiac CT have not yet been developed. The findings will help fill this gap by providing practical data to guide dose monitoring and optimisation.

By contributing to the groundwork for setting local DRLs, this study supports broader efforts to improve radiation safety in line with international recommendations, such as those from the International Commission on Radiological Protection (ICRP). The results are expected to assist radiologists, medical physicists, and healthcare policymakers in improving cardiac imaging protocols, enhancing patient safety, and guiding the development of institutional or even national dose reference standards

#### 1.6 Scope and Limitations

This study focused on assessing radiation dose levels and identifying dose-scanning parameters in cardiac CT imaging at HPUSM. The analysis was based on retrospective data collected from 200 adult patients who underwent cardiac CT examinations between May and December 2024, using two different CT scanners: the Siemens SOMATOM Definition AS+ and the Philips Incisive CT. The scope was limited to specific scan protocols relevant to coronary artery evaluation, namely CorCTA, CorCTAAdapt, and CTA Coronary.

Only adult patients aged 18 years and above with complete scan records and appropriate clinical indications related to cardiac conditions were included. Cases were excluded if they involved imaging protocols outside the study scope, incomplete or missing dose data, unavailable images in the PACS system, or a lack of documented medical records. Additionally, patients with abnormal anatomical findings such as heavily calcified coronary arteries, which may introduce inconsistencies in dose measurement, were also excluded.

As the study used retrospective secondary data, it was subject to limitations in terms of patient selection and imaging parameter control. This research did not involve any assessment of image quality or diagnostic accuracy, as its primary aim was to establish typical dose values and investigate scanning parameters contributing to dose variation. Therefore, clinical outcomes were beyond the scope of this work.

#### 1.7 Thesis Organisation

This thesis is structured into five chapters to provide a clear and logical presentation of the research process and findings.

Chapter 1 introduces the background of the study, outlines the problem statement, research objectives, significance of the research, scope and limitations, and provides an overview of the thesis structure. Chapter 2 reviews relevant literature, including the principles of cardiac CT, radiation dose metrics, and related studies on diagnostic reference levels and dose variation in CT imaging. This chapter establishes the theoretical framework and supports the rationale for the current research.

Chapter 3 explains the methodology employed in the study, including descriptions of the CT scanners used, data sources, selection criteria, and the statistical methods used to analyse the data. It also details how the typical dose and local diagnostic reference levels were determined. Chapter 4 presents and discusses the results of the study, including typical dose values for each protocol, proposed diagnostic reference levels, and statistical relationships between scanning parameters and radiation dose indicators.

Chapter 5 concludes the study by summarising the key findings, reflecting on the research objectives, and offering recommendations for future work and improvements in cardiac CT practice.

#### **CHAPTER 2**

#### LITERATURE REVIEW

This chapter provides an overview of the key concepts and previous findings related to cardiac CT imaging and radiation dose. It begins with the basic principles of how CT works, including image formation, data acquisition, and reconstruction techniques. It then focuses on how radiation dose is measured in CT using standard metrics like CTDI and DLP, and explains the role of typical dose and Diagnostic Reference Levels (DRLs) in improving radiation safety.

The chapter also reviews common scanning modes used in cardiac imaging, and discusses how factors such as age, gender, tube current, exposure time, and scan length can influence radiation dose. These insights help to support the purpose of this study in establishing typical dose levels and identifying scanning parameters that contribute to dose variations in cardiac CT.

#### 2.1 Basic Principles of Computed Tomography (CT)

#### 2.1.1 X-ray Attenuation Through an Object

X-ray imaging relies on the principle of attenuation, wherein X-rays propagating through a sample are either absorbed or transmitted to a detector. The general expression for X-ray attenuation follows the exponential decay law (Jung, 2021):

$$I = I_0 \cdot e^{-\mu x}$$
 Equation 1

where  $I_0$  is the initial X-ray intensity before interaction with the object,  $I_x$  is the intensity after passing through the material,  $\mu$  is the linear attenuation coefficient, and x represents

the thickness of the absorbing medium. This relationship is a mathematical representation of how materials of different densities and thicknesses attenuate X-rays differently.

When X-rays traverse multiple layers of material with varying attenuation properties, the transmitted intensity is described by an extended form of the Lambert–Beer law (Jung, 2021):

$$I = I_0 \cdot e^{-(\mu_1 + \mu_1 + \mu_3 + \mu_4)x}$$
 Equation 2

This formulation indicates that the total attenuation is additive, and the total linear attenuation coefficient ( $\mu_{tot}$ ) equals the sum of individual coefficients  $\mu_{tot}=\mu_1+\mu_2+\mu_3+\mu_4$  (as shown in Figure 1). Consequently, the intensity captured by the detector is proportional to the integral of the object's two-dimensional transparency and corresponds to the cumulative linear attenuation along the X-ray path (Jung, 2021).

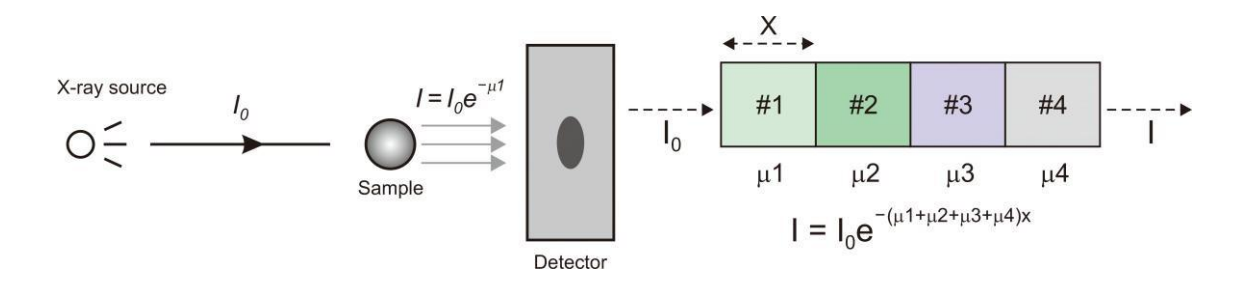


Figure 2.1: X-ray beam attenuations passing through of an object (left) and intensity of an X-ray beam passing through an object with multiple different linear attenuation coefficients ( $\mu$ 1,  $\mu$ 2,  $\mu$ 3,  $\mu$ 4) (right) (Jung, 2021).

#### 2.1.2 Image Data Acquisition

Computed tomography (CT) imaging involves the acquisition of cross-sectional images of an object by rotating an X-ray source around it. During the scan, the subject is placed on a table while the X-ray source, located within the gantry, rotates and emits X-rays through the object. Detectors on the opposite side collect the transmitted X-rays. These signals are processed by the data acquisition system (DAS) to generate projection data, which are essential for image reconstruction (Jung, 2021).

The reconstruction of a CT image requires X-ray projections obtained at multiple angles, typically covering 360° or 180° rotations. For accurate image formation, two critical conditions must be met: (a) the object must appear in every projection dataset to ensure consistency across all angles, and (b) the object must remain still throughout the scan to avoid motion artefacts. These requirements are fundamental to producing precise and high-quality tomographic images (Jung, 2021).

#### 2.1.3 CT Image Reconstruction

CT image reconstruction is a mathematical process used to determine the 2D attenuation map f[f(x,y)] of an object from multiple 1D X-ray projections  $[P(r,\theta)s]$ . These projections, collected at various angles during a single rotation, form a sinogram, which represents the raw data used for image reconstruction (Jung, 2021).

According to Jung (2021), several methods exist for reconstruction, including simple and filtered back projection, matrix inversion, iterative techniques, and Fourier transform methods. The filtered back projection (FBP) method, introduced to overcome blurring from basic back projection, has been widely used despite its susceptibility to noise. Iterative reconstruction (IR), originally used in the 1970s, has regained attention

due to its improved accuracy by repeatedly adjusting estimates to match measured projections. The central slice theorem (CST) connects the Radon transform of an object with its 2D Fourier transform, enabling accurate reconstruction by converting sinogram data  $P(r, \theta)$  into the frequency domain and applying inverse Fourier transform to recover the attenuation distribution f(x, y).

#### 2.1.4 CT Numbers/Hounsfield Units

According to Jung (2021), CT images are digital representations composed of a matrix of pixels, where each pixel corresponds to a voxel such as a volume element defined by the pixel area and slice thickness. The voxel size is influenced by the matrix dimensions, field-of-view (FOV), and section thickness. Each pixel holds the average linear attenuation coefficient of the tissue at its spatial location, and these values are transformed into grayscale intensities for image display.

Standard CT images typically use a 512×512 matrix with 12-bit depth (4,096 grey levels), though higher resolutions, such as 1,024×1,024 or 2,048×2,048, are now available in ultrahigh resolution CT. The CT number or Hounsfield Unit (HU) quantifies the pixel attenuation relative to water, calculated as shown in the equation below (Jung, 2021):

$$\mu_{pixel} - \mu_{water} \qquad \qquad \text{Equation 3}$$

$$CT \ Number \ (HU) = 1000 \times \underline{\qquad}$$

$$\mu_{water}$$

Figure 2.2 illustrates the Hounsfield Unit (HU) scale used in computed tomography (CT) to distinguish between different tissue densities. Water is assigned a reference value of 0 HU, while air is given –1000 HU. Tissues denser than water, such as bone and blood, have positive HU values, whereas less dense tissues, such as fat and lung, have negative values. This scale aids in the identification and characterisation of anatomical structures based on their attenuation properties (Jung, 2021).

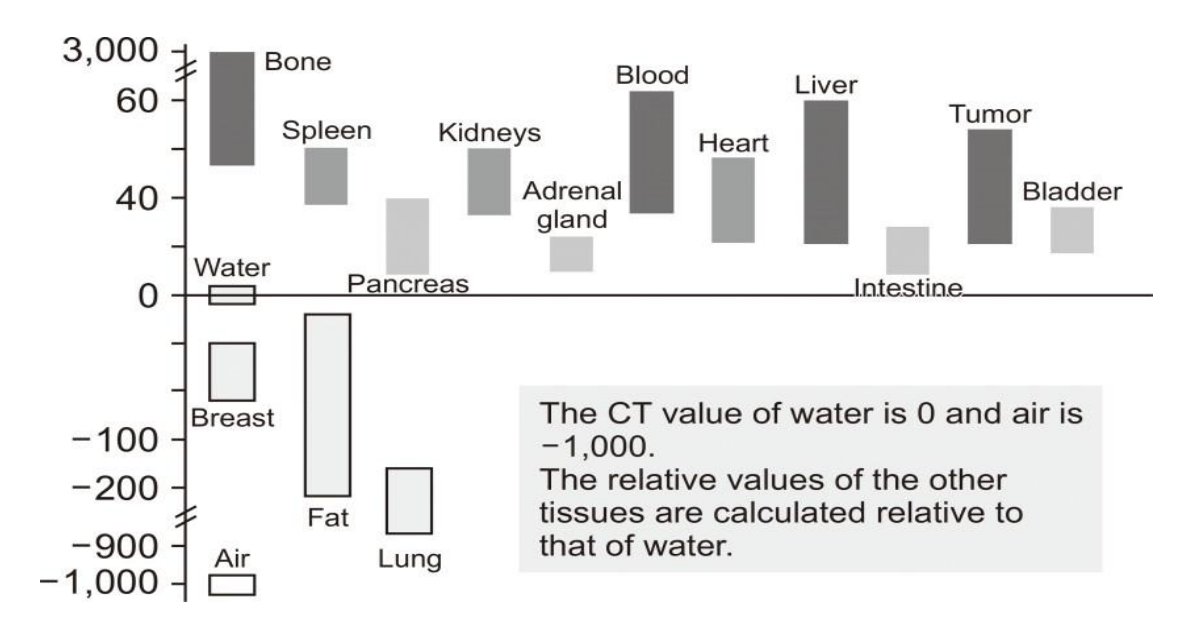


Figure 2.2: Range of Hounsfield Unit (HU) scale of computed tomography (CT) numbers for various tissues (Jung, 2021).

By this definition, water has a CT number of 0 HU and air -1,000 HU, providing a standardised scale for differentiating tissue densities.

#### 2.1.5 Components of CT Scanner

According to Jung (2021), modern CT scanners are composed of several integrated systems, including the gantry, patient couch, operating console, and image reconstruction computer. The gantry houses essential imaging components such as the X-ray tube, high-voltage generator, filters, collimators, detector arrays, and the data acquisition system (DAS). The CT X-ray tube typically operates at 60–80 kW for up to 20 seconds and produces high-resolution imaging using a small focal spot size (approximately 1.3×10 mm). A three-phase generator supplies high voltage, typically between 120–140 kV, and its power capacity in kilowatts determines the scanner's exposure parameters, including tube voltage (kV) and tube current (mA).

Filters is positioned between the X-ray tube and the patient eliminate low-energy X-rays that do not contribute to image formation but increase patient dose. Collimators are located after the filter that has the function to shape the X-ray beam to the desired slice thickness and reduce scatter radiation, improving image quality and minimizing unnecessary exposure (Jung, 2021).

CT detectors are typically gas-filled or solid-state (scintillation) detectors. Gas detectors use pressurized noble gases like xenon or krypton (around 25 atm) and are segmented into subdetectors. Earlier systems used sodium iodide (NaI) scintillation crystals coupled with photomultiplier tubes. Modern solid-state detectors convert X-rays into visible light via scintillating crystals, and photodiodes then convert this light into electrical signals for image processing (Jung, 2021).

The CT patient couch is made of low-absorption carbon fiber to support patient positioning and movement through the gantry during scanning. It must be strong and rigid, capable of supporting up to 204 kg. In diagnostic CT, the couch has a rounded top for patient comfort, whereas in radiation therapy, a flat couch is used to replicate treatment positioning accurately (Fan et al., 2024).

#### 2.1.6 Scanning Mode in Cardiac CT

Cardiac CT imaging requires precise synchronisation with the cardiac cycle due to the rapid and complex motion of the coronary arteries. To reduce motion artefacts, ECG-gated scanning techniques are used, primarily divided into retrospective and prospective ECG-gating (Fan et al., 2024).

Retrospective ECG-gating involves continuous helical scanning with X-ray exposure throughout the cardiac cycle. This allows flexible image reconstruction at different phases and enables cardiac function analysis. However, it results in a higher radiation dose. To mitigate this, ECG-based tube current modulation can be applied, increasing the tube current during optimal imaging windows (usually in diastole) and reducing it elsewhere. While effective for dose reduction, up to 37%, it is not suitable for patients with irregular heart rhythms due to the fixed timing of current modulation (Fan et al., 2024).

Prospective ECG-gating, in contrast, uses an axial "step-and-shoot" approach where the scanner acquires data only at specific cardiac phases, typically late diastole, with no exposure during table movement. This significantly reduces radiation dose, up to 72% in paediatric studies (Tang et al., 2021) without compromising image quality—provided the heart rate is stable and low (≤ 65 bpm). The main limitation is the inability to assess

cardiac function due to limited phase coverage, and greater susceptibility to motion artefacts at higher or irregular heart rates (Fan et al., 2024).

#### 2.2 CT Dosimetry

#### 2.2.1 Computed Tomography Dose Index (CTDI)

The Computed Tomography Dose Index (CTDI) is a standardised metric developed to characterise the radiation output of CT scanners. It allows for dose comparison across scanners and protocols but does not represent the actual dose absorbed by patients. There are three primary forms of CTDI: CTDI 100, CTDI w and CTDIvol (Zhao et al., 2022). CTDI 100 is derived from dose measurements over a 100-mm length using a pencil-type ionisation chamber in a polymethyl methacrylate (PMMA) phantom. CTDI w averages these measurements using a one-third to two-thirds weighting of the centre and peripheral values to represent dose uniformity across the scan plane, while CTDIvol adjusts CTDI for helical scanning using the pitch factor.

Although CTDI<sub>vol</sub> is widely used and typically displayed on scanner consoles, it does not account for patient size, anatomy, or tissue sensitivity. CTDI<sub>vol</sub> is also used in regulatory compliance, where institutions are required to ensure that displayed values remain within  $\pm 20\%$  of actual measurements for key protocols (Zhao et al., 2022).

Fan et al. (2025) highlighted limitations of CTDI 100 in wide-beam CT, noting that its 100-mm integration length is inadequate for capturing all primary and scattered radiation. Their use of radiochromic film demonstrated that dose measurement efficiency drops significantly with beam widths of 80–160 mm, necessitating correction factors to improve dose accuracy in such systems.

In dental CBCT imaging, (Mauro and Costa, 2021) reported that CTDI<sub>100</sub> is insufficient for large field-of-view (FOV) protocols, as it often captures less than 70% of the true dose. Their study introduced CTDI<sub>300</sub> measured over 300 mm, as a more accurate representation of radiation exposure in these applications. The modified efficiency approach they proposed supports the adoption of extended-length measurements in dosimetry for large-FOV imaging.

#### 2.2.1 Dose-Length Product (DLP)

Dose-Length Product (DLP) is calculated as shown in the below equation (Zhao et al., 2022):

$$DLP = CTDI_{vol} \times scan \ length$$
 Equation 4

The Dose-Length Product (DLP) is a radiation dose descriptor that extends the information provided by the  $CTDI_{vol}$  by incorporating the scan length along the z-axis (Zhao et al., 2022). It is calculated by multiplying the  $CTDI_{vol}$  by the scan length, providing an approximation of the integrated dose along the scanned region. Clinically, the DLP is used to indicate the overall energy imparted by a given scan protocol. It is expressed in milligray-centimetres (mGy·cm), emphasizing its role as a product of dose intensity and scan length (Zhao et al., 2022).

Then, the study further elaborated that dividing DLP by the nominal beam width to back-calculate CTDI can be misleading in wide-beam settings. If the scan height exceeds the chamber length or includes scattered radiation tails not accounted for in  $CTDI_{100}$ , this calculation may significantly misrepresent the actual exposure.

In modern systems, especially wide-detector scanners, Fan et al. (2025) demonstrated that console-displayed DLP values tend to underestimate total dose compared to extended-length film-based measurements. They proposed correction factors for both  $CTDI_{vol}$  and DLP in head and body phantoms, especially important for beam widths  $\geq$ 100 mm (Fan et al., 2025).

### 2.3 Coronary Computed Tomography Angiography (CCTA)

CCTA is a non-invasive imaging modality increasingly used in clinical settings to evaluate coronary artery disease. According to the study Tekinhatun et al. (2024), CCTA examinations are conducted using a dual-source CT scanner equipped with a 128 × 2-slice configuration and two X-ray tubes aligned at a 95° angle (Somatom Definition Flash, Siemens Healthcare, Germany). This advanced scanner design allows for high temporal resolution and efficient image acquisition, which are critical for imaging dynamic structures such as the heart.

The imaging protocol begins with the acquisition of non-contrast images for Coronary Artery Calcium Score (CACS), which is performed using the Agatston method. These initial images are acquired with a slice thickness of 3 mm using a prospective ECG-triggered scan at 120 kVp. This step not only quantifies the calcium burden but also provides detailed anatomical images of the entire thoracic cavity through the use of a wide field of view (FOV), thereby enabling the identification of extracardiac findings that may be clinically relevant (Tekinhatun et al., 2024)

#### 2.4 Radiation Dose Distribution in Patient Demographic (Age and Gender)

Age and gender influence the absorbed radiation dose due to differences in body composition and radiation sensitivity. According to study by Fan et al. (2024), it acknowledged that paediatric and younger patients, particularly females, are more sensitive to radiation. Therefore, dose reduction techniques such as low tube voltage scanning (e.g., 80–100 kV), especially for nonobese patients, are strongly encouraged in these populations (Fan et al., 2024).

According Saleh et al. (2023), the study found that the mean DLP and CTDI<sub>vol</sub> values were higher for females compared to male patients. The study reported that the mean DLP was  $640.86 \pm 417.69$  mGy.cm for females and  $623.29 \pm 288.98$  mGy.cm for males. Mean CTDI<sub>vol</sub> for females is higher which wass  $14.766 \pm 8.21$  mGy compared to the males ( $12.51 \pm 4.73$  mGy). Furthermore, the CTDI<sub>vol</sub> mean organ doses for older age groups were higher than younger age groups, with statistically significant differences (p < 0.001). This means that older patients tend to have higher radiation doses in CT examinations compared to younger patients.

In a retrospective study by Szarmach et al. (2025), radiation dose values were analysed in 247 adult patients undergoing abdominal and pelvic CT examinations. The study included 113 female and 134 male patients. The average CTDI<sub>vol</sub> for the entire cohort was 11.37 mGy. When analysed by sex, females had a slightly higher CTDI<sub>vol</sub> of 11.61 mGy, compared to 11.17 mGy in males. This difference indicates that female patients received marginally more radiation per slice of the scan.

The DLP, averaged 514.88 mGy·cm across all patients. DLP values were 508.35 mGy·cm in females and 520.38 mGy·cm in males. Although male patients had a slightly higher total DLP, this is likely due to their generally taller stature and, consequently, longer scan ranges (Szarmach et al., 2025).

#### 2.5 Scanning Parameters Influencing Radiation Dose in CT Imaging

#### 2.5.1 Exposure Time and Scan Length

Exposure time and scan length are directly related to the overall radiation dose during CCTA. Longer scan durations and extended z-axis coverage typically result in higher radiation doses, especially in retrospective ECG-gated modes where the tube is active over several cardiac cycles. In contrast, prospective ECG-gated axial scanning significantly limits exposure time by activating the X-ray beam only during predetermined cardiac phases, thus reducing dose substantially, particularly in patients with low and stable heart rates (Fan et al., 2024).

Wide-detector CT scanners with 160 mm z-axis coverage enable imaging the entire heart in a single cardiac cycle, minimizing scan length and exposure time. These systems eliminate stair-step artifacts and reduce cumulative exposure from multiple heartbeats, especially in patients with regular rhythms (Fan et al., 2024).

Exposure time also significantly influences radiation dose, particularly through the choice of scanning mode. In retrospective ECG-gated scans, the patient is exposed to X-rays throughout the entire cardiac cycle, leading to longer exposure times and increased CTDI<sub>vol</sub> and DLP. In comparison, prospective ECG-triggered scans restrict radiation to specific cardiac phases, most commonly diastole, thereby reducing overall exposure time and dose. ECG-based tube current modulation further enhances this

approach by delivering full radiation only during target phases and minimizing it during others, effectively reducing CTDI<sub>vol</sub> by up to 50% without a significant loss in image quality.

However, this technique is most effective in patients with stable and slower heart rates, as irregular rhythms can compromise timing accuracy and image interpretability (Kędzierski et al., 2023).

Even with a moderate C CTDI vol, an unnecessarily long scan can substantially elevate DLP. For instance, one imaging centre reported very high DLP values due to extended scan lengths despite using a relatively low CTDIvol of 33.1 mGy. Studies have shown that limiting the scan to the clinically relevant region can reduce DLP by up to 70%, emphasizing the need for precise protocol planning and adherence (Kędzierski et al., 2023).

### 2.5.2 Tube Current (mA) and Exposure Time (s)

The product of tube current and exposure time (mAs) determines the amount of radiation used per slice, which directly influences CTDI vol. Increased mAs improves image quality but proportionally raises CTDI vol.

The tube current (measured in mAs) is another determinant of radiation dose. Higher mAs values improve image quality by reducing noise but increase patient dose. Manufacturers have implemented automatic exposure control systems such as Smart mA and Sure. Exposure to modulate tube current based on patient size and anatomy, effectively lowering mAs without compromising image quality (Fan et al., 2024).

Furthermore, iterative reconstruction (IR) algorithms, including ASIR, AIDR3D, and model-based IR, allow for dose reductions by enabling diagnostic-quality imaging at lower mAs settings. Deep learning reconstruction (DLR) techniques further enhance image quality at lower doses, offering significant radiation reduction opportunities (Fan et al., 2024).

The Study by Rehani et al. (2020) reported that automatic exposure control (AEC), which adjusts mA based on patient size and attenuation, helps modulate CTDI<sub>vol</sub> and reduce unnecessary dose.

A study by Kędzierski et al. (2023) that was conducted across several centres, found that using fixed high mAs settings regardless of patient size resulted in unnecessary dose escalation, with DLP values as high as 3277 mGy·cm. In contrast, individualized mAs settings and the use of automatic exposure control (AEC) allow for significant dose reduction without compromising image quality. For example, the PROTECTION VI study showed that with optimised modeling tube current settings, median DLP values as low as 195 mGy·cm could be achieved.

A Study by Yang (2020) showed that tube current (mAs) lowers noise and improves image quality but higher settings increase dose unless modulated by Automatic Tube Current Modulation (ATCM) systems.

#### 2.6 Radiation Dose Management in Cardiac CT

Monitoring radiation dosage in CT, particularly in cardiac imaging, is critical due to the risks associated with excessive exposure. The ICRP established DRLs in the 1990s to optimise radiation exposure while ensuring diagnostic quality. DRL often set at the 75th percentile of dose distributions, function as benchmarks for monitoring procedures

and indicating areas for enhancement. These thresholds operate as benchmarks for optimisation instead of dose limitations, improving patient safety while retaining imaging quality (Razali et al., 2019).

#### 2.7 Typical Dose (50th Percentile)

The typical dose is defined at 50th percentile of the dose distribution, signifies the median radiation dose given to patients during standard imaging procedures. Unlike the 75th percentile used for DRLs, the 50th percentile signifies the dose most patients receive under normal conditions, excluding outliers.

For example, reported median CTDI<sub>vol</sub> and DLP values of 13 mGy and 166 mGy·cm, respectively, for cardiac CT in Australia. This highlights the effectiveness of dose reduction strategies like prospective ECG gating, which significantly lowered doses compared to retrospective gating.

Similarly, Razali et al. (2019) underscored the significance of typical doses in establishing local diagnostic reference levels (LDRLs), providing a benchmark standard procedure.

#### 2.8 Establishing Local Diagnostic Reference Levels (LDRLs)

When it comes to cardiac CT imaging, DRLs is important to analyse and improve radiation doses. They enable comparisons of local practices against established benchmarks, which encourages lower doses while keeping diagnosis quality high.

Similarly, Rawashdeh et al. (2019) conducted DRLs for Cardiac CT in Jordan by collecting dose data (CTDI<sub>vol</sub> and DLP) from cardiac CT scan across seven hospitals. The 75<sup>th</sup> percentile values were used to determine DRLs. The results for the study highlighted higher DRLs of 47.7 mGy (CTDI<sub>vol</sub>) and 1035 mGy·cm (DLP), reflecting technological differences and procedural variations across regions.

Additionally, Razali et al. (2019) conducted a retrospective study on patients undergoing CT scans for multiple anatomical regions at Advanced Medical and Dental Institute (AMDI). The study established institutional diagnostic reference levels (DRLs) for combined anatomical CT regions at AMDI. CT of Thorax, Abdomen, and Pelvis (TAP) was the most frequently performed examination. Dose values for multiphasic studies were higher, with a reported average of 1300 mGy.cm for multiphasic TAP, and local values were generally lower than international DRLs except for multiphasic TAP studies.

In Saudi Arabia, Alhailiy et al. (2018) collected data from 11 hospitals across Saudi Arbia and a total of 197 CCTA were analysed. The study found dose variability due to the variations in doses due to differences in scanning protocols, equipment, and patient weight. Patient doses were measured for CTDI<sub>vol</sub> and DLP using two ECG-gating methods (prospective and retrospective). The study established NDRLs for CCTA in Saudi Arabia: CTDI<sub>vol</sub> and DLP for prospective gating were 29 mGy and 393 mGy.cm, and for retrospective gating, they were 62 mGy and 1057 mGy.cm. The results showed

that radiation doses were lower than those in Europe, due to the use of dose-saving technologies. These findings not only highlight the variability in practice but also emphasize the need for benchmarking and standardisation to optimize dose management.

In Australia, a study conducted a retrospective study where they collected the data via questionnaire from 11 hospitals across the Australia. A total of 338 patients' data were analysed, highlighting the CT dose parameters such as CTDI<sub>vol</sub> and DLP for CCTA and CACS. The national diagnostic reference levels (NDRLs) for CCTA in Australia were proposed as 22 mGy for CTDI<sub>vol</sub> and 268 mGy cm for DLP, with the CS test DLP at 137 mGy cm. The study also emphasized lower DRLs than most international studies due to dose-saving technologies, such as prospective ECG-gated modes and iterative reconstruction algorithms (Alhailiy, Ekpo et al., 2018).

Mafalanka et al. (2015) reported DRLs for coronary computed tomography angiography (CCTA) in France through a retrospective analysis of 460 CCTA scans performed over 3 months in 8 French Hospital using 64-to-320 detector CT scanners. The results for the study are 26 mGy (CTDI<sub>vol</sub>) and 370 mGy·cm (DLP) for prospective ECG gating, and 44 mGy and 970 mGy·cm for retrospective gating. The study also highlighted the significant impact of acquisition techniques on dose optimization.